International Journal of Marine Energy 15 (2016) 56–67

Contents lists available at ScienceDirect

International Journal of Marine Energy

journal homepage: www.elsevier.com/locate/ijome

Experimental investigation of mooring configurations for wave energy converters

Guilherme Moura Paredes [a,*], Johannes Palm [b], Claes Eskilsson [b], Lars Bergdahl [b], Francisco Taveira-Pinto [a]

[a] Faculdade de Engenharia, Universidade do Porto, Rua Dr. Roberto Frias, s/n, 4200-465 Porto, Portugal
[b] Department of Shipping and Marine Technology, Chalmers University of Technology, Gothenburg, Sweden

ARTICLE INFO

Article history:
Received 17 March 2016
Accepted 21 April 2016
Available online 22 April 2016

Keywords:
Wave energy converters
Moorings
Physical model
Experiment
Cables
Wave tank
Compact moorings
Catenary

ABSTRACT

Mooring systems are required to keep floating wave energy converters (WECs) on station. The mooring concept might impact the performance of the WEC, its cost and its integrity. With the aim of clarifying the pros and cons of different mooring designs, we present the results from physical model experiments of three different mooring concepts in regular and irregular waves, including operational and survival conditions. The parameters investigated are the tension in the cables, the motions of the device in the different degrees of freedom and the seabed footprint in each case. We can see that the mooring system affects the performance of the wave energy converter, but the magnitude of the impact depends on the parameter analysed, on the mode of motion studied and on the conditions of the sea. Moreover, different configurations have similar performances in some situations and the choice of one over another might come down to factors such as the type of soil of the seabed, the spacing desired between devices, or environmental impacts. The results of our experiments provide information for a better selection of the mooring system for a wave energy converter when several constraints are taken into account (power production, maximum displacements, extreme tensions, etc).

1. Introduction

A good mooring system for a floating wave energy converter must not only ensure the survivability of the device, but also account for its effects on the motions and on the power take-off. Furthermore, the moorings should be easy to monitor and maintain, while minimising material and installation costs. It is also desirable that the mooring system takes as little space as possible on the seabed, in order to allow the devices to be installed close to each other in parks, something that usually is not important or allowed for other offshore structures.

Because of the differences between wave energy converter concepts, the mooring system employed must be tailored to the particular needs of each technology concept. Therefore, varied solutions for mooring systems of wave energy converters have been proposed. The diversity of solutions occurs even for similar devices. For example, in [1] a mooring system composed of taut synthetic cables is suggested for the FLOW wave energy converter, a hinged attenuator, while in [2], the standard chain catenary is used for the DEXA, another hinged attenuator. The catenary is also used in the South West Mooring

* Corresponding author.
E-mail address: moura.paredes@fe.up.pt (G. Moura Paredes).

http://dx.doi.org/10.1016/j.ijome.2016.04.009
2214-1669/

Test Facility [3] and in numerical simulations of point absorbers [4]. It is a standard solution due to its long use in the offshore industry, but it might not be the best for wave energy converters.

There are also examples of possible conflicting results from mooring studies pertaining to motion dependent devices. In [2], the experimental results show that the pre-tension of the catenary mooring cables, in the range that was tested, can lead to variations of up to 16% in power extraction. In [5] it is concluded that the catenary is not at all an efficient way to moor point absorbers. The reasons for this are the large weight of the catenary (leading to high material costs), its large seabed footprint (which prevents close installation in parks) and its high damping levels (reducing the conversion efficiency). However, for the case simulated in [6] (within the limitations of the numerical model used) it is concluded that the catenary mooring system has little to no influence on the power extraction: less than 1%. For motion independent devices, for example, terminators like the WaveDragon [7], the influence of the mooring system might be residual.

Due to the variability of solutions and conclusions, we aim to clarify the benefits and the impacts that different mooring concepts might have on point absorbers. For that we tested three different configurations in small scale models, Fig. 1: (i) a compact (small seabed footprint) configuration consisting of a synthetic cable and a floater; (ii) a compact configuration composed of a synthetic cable, a floater and a clumpweight in a zig–zag geometry; and (iii) the catenary, as the industry standard solution. The tests were conducted at the Hydraulics Laboratory of the Faculty of Engineering of the University of Porto.

The compact configurations were inspired by results and ideas presented in [5,8] where the impact of different mooring configurations for wave energy converters was analysed. One of the configurations studied had an intermediate floater, which decoupled the horizontal mooring loads, caused by the horizontal motions of the wave energy converter, from the vertical loads, induced by the heave and pitch motions. Another configuration used a clumpweight and a floater, resulting in a compliant configuration with a smaller footprint than the catenary, but still with significant inertia.

The performance of the mooring configurations is assessed based on their impact on the motions of a buoy in surge, heave and pitch, and on the measured tension forces in the cables.

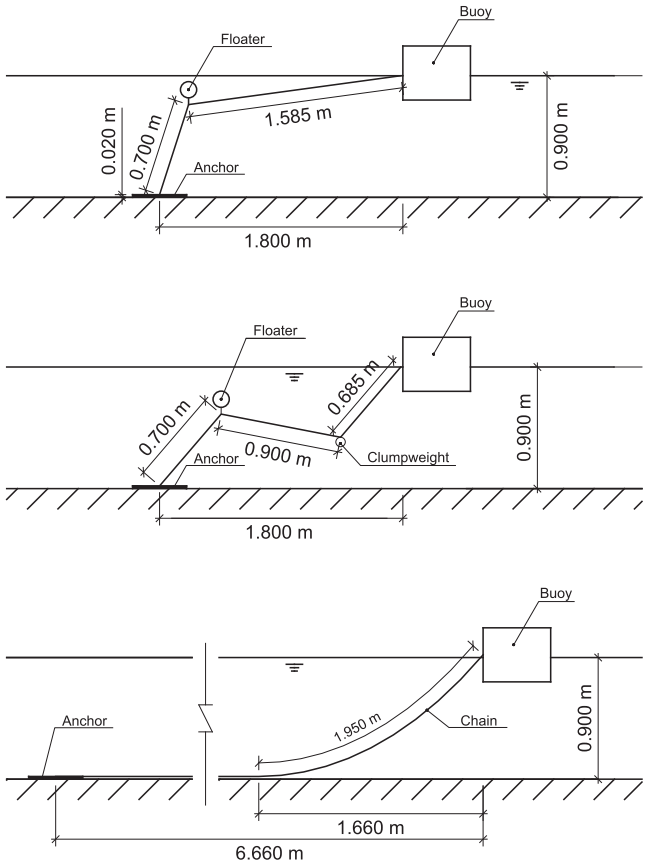

Fig. 1. Schematics and dimensions of the mooring legs of the tested configurations. Top: synthetic cable and floater (CON1); middle: synthetic cable, floater and clumpweight (CON2); bottom: catenary.

We will show that the mooring concepts tested have an impact on the behaviour of the device and that they affect it differently. We will also show that, in terms of station-keeping and mooring loads, the concepts have varying performances and that, overall, the catenary might be an inefficient choice, as stated in [5].

Although the study focuses on WECs, no power take-off was modelled in the tests. An active power take-off system increases the loads in the mooring cables and the surge displacements, as explained in [9] and reported in [10]. However, at the small scale used, the power take-off is cumbersome to simulate in a quantifiable way. Moreover, introducing a power take-off would restrict the conclusions of the experiments to devices with the specific power take-off modelled, when the goal of our work is to study the effect of mooring configurations alone.

The results presented here are part of a larger set of tests, including variations on the pre-tension of each configuration for sensitivity analysis. That data will be presented in future publications.

2. Experimental work

2.1. Buoy and mooring design

The physical model was composed of a cylindrical buoy kept on station by three mooring legs spaced 120°, Fig. 2. The three-leg arrangement is advantageous when used in arrays, as it allows a high concentration of devices and the possibility of anchors to be shared by several devices. Such an arrangement is studied in [3] using catenaries, and in [10] using a configuration with a floater similar to the one presented in this work for an array of point absorbers. (see Fig. 3)

The extreme conditions used in the design of the mooring system and in the survivability tests were the sea-states for the Portuguese Pilot Zone (offshore Figueira da Foz, Portugal). These were determined in [1] for the design of the mooring system of the FLOW wave energy converter, and are listed in Table 1 as SURV1 and SURV2. A JONSWAP spectrum with a shape parameter $\gamma = 3.3$ was used to represent the irregular sea-states. The peak periods (T_P) of the survival sea-states were estimated from the zero-crossing periods (T_z) given in [1] using the relation $T_P = 1.287\,T_{02} = 1.287\,T_z$. The period $T_{02} = \sqrt{m_0/m_2}$, where m_0 and m_2 are the first and second order spectral moments, is an approximation to T_z for narrow-banded spectra [11].

Operational conditions were also tested using the wave statistics from [12] for the region offshore Figueira da Foz. Two sea-states were defined selecting the conditions with most available energy (combined power and probability of occurrence), listed in Table 1 as OP1 and OP2. The water depth was also based on the conditions presented in [1]: 90 m.

Froude similarity was used to scale down the model with a geometrical scale of $\lambda_l = 1/100$, resulting in the model sea-states of Table 1 and a water depth of 0.900 m. The scale $\lambda_l = 1/100$ was selected because of the limitations of the wave generator for larger waves at bigger scales. However, at this scale, the dimensions of a buoy simulating a reasonably sized wave energy converter would be too small for the tension in the cables to be measured with good enough accuracy. To increase the

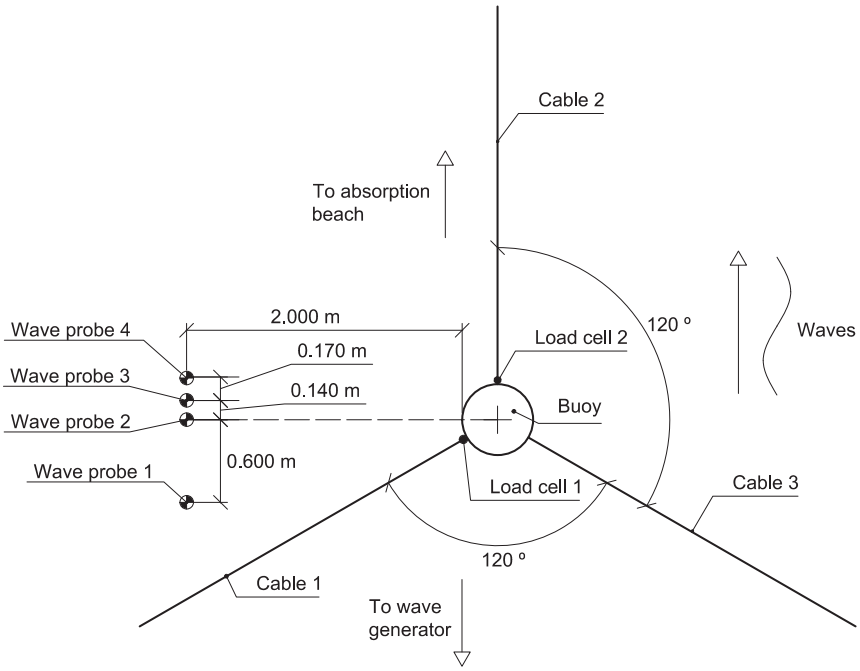

Fig. 2. Top view of the experimental setup.

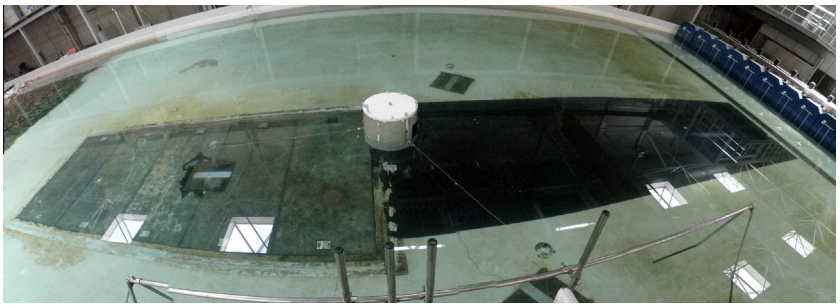

Fig. 3. Panorama of the experimental set-up.

Table 1
Irregular sea-states. H_s – significant wave height; T_z – zero-crossing period; T_P – peak period; OP – operational sea-state; SURV – survival sea-state.

Type	Prototype			Model	
	H_s (m)	T_z (s)	T_P (s)	H_s (m)	T_P (m)
OP1	3.0	–	9.0	0.030	0.9
OP2	3.0	–	13.0	0.030	1.30
SURV1	8.6	9.0	11.6	0.086	1.16
SURV2	9.5	11.0	14.2	0.095	1.42

magnitude of the tension forces in the cables and ensure the accuracy of the measurements, a scale $\lambda_l = 1/50$ was used for the buoy, twice the scale of the remaining components of the model.

The mooring configurations were designed to resist the slowly varying loads, while being compliant with the wave frequency motions. Current and wind loads were not accounted for in the design as they could not be simulated in the wave tank. The catenary was designed following the guidelines and design procedures presented in [13,14]. For the compact mooring configurations there was no design guideline or method available. As such, the basis for their design was to achieve approximately the same secant stiffness as the catenary under the action of the slowly varying loads (the same horizontal reaction force at the maximum allowed slowly varying displacement). This way it is possible to have a fair comparison between the three different configurations.

In order to limit the factors that might induce unexplained variability in the results, in the compact configurations the length of the different segments of cable, the distance from the anchoring point to the buoy and the buoyancy of the floaters were the same. Additionally, for symmetry reasons, the submerged weight of the clumpweights had the same magnitude as the buoyancy force of the floaters. To take advantage of the dimensions of these configurations, the distance from the anchor to the buoy was set to be twice the water depth, 1.800 m.

The main restrictions in the design of the compact mooring configurations is to guarantee that the floaters stay submerged at all times and that the clumpweights never come to rest on the bottom. If any of these situations occur, there will be a sudden decrease in restoring force and tension in the cables, resulting in large displacements of the buoy and, likely, snap loads.

In the following discussion, the configuration with synthetic cables and floaters will be termed CON1 and the configuration with synthetic cables, floaters and clumpweights will be termed CON2.

2.2. Experimental setup

The hull of the buoy was made of fibre-reinforced plastic with an inner ballast made of rubber; its properties, *excluding any extra fixture or adapter*, are presented in Table 2. The centre of gravity and the inertia around horizontal axis through the centre of gravity were determined using the procedures described in [15]. Adapters were bolted on the sides of the buoy to attach the mooring cables, in a position 0.222 m from the top of the buoy and 0.015 m from the hull. The mass of the adapters was 0.0572 ± 0.0018 kg.

Table 2
Properties of the buoy. D – diameter; h – height; I_{xx} – inertia around the horizontal axis through the centre of gravity; C_g – centre of gravity (distance from the top).

Mass	D	h	I_{xx}	C_g
35.50 ± 0.05 kg	0.515 ± 0.002 m	0.401 ± 0.002 m	0.87 ± 0.02 kg·m^2	0.3247 ± 0.0003 m

Hollow acrylic spheres were used for the floaters and lead fishing weights were used for the clumpweights. Table 3 summarises the properties of the floaters and Table 4 the properties of the clumpweights.

The chain used in the catenary was selected so that it had reasonable properties in comparison with the dimensions of the model. It was made of zinc plated steel and its characteristics are presented in Table 5. Following the design procedures mentioned above, the horizontal span required for the catenary cables was 5.737 m. However, for practical reasons (to anchor the chains at the walls of the wave tank), the span of the catenaries was increased by 0.923 m to 6.660 m. This extra length of cable has little to no influence in the experiments, since it will be resting on the floor. Moreover, since the span of the catenary without the extension was already much larger than the span of the compact configurations, the added length will not change the rating of the configurations when it comes to size.

The cables in the compact mooring configurations were made of polyester with a braided sheath and a parallel strand core. Its properties are presented in Table 6. This type of cable was chosen because it had negligible extension in the range of tension forces anticipated, so that elasticity would not be a significant variable in the outcome of the experiments. The objective of the tests was to assess the behaviour of the configurations under wave loading due to changes in their geometry.

The stiffness of the synthetic cables and of the chain was measured in tensile tests where five samples of each were loaded up to the breaking point. The slope of the initial linear portion of each force-elongation curve was then determined and their mean values are presented in Tables 5 and 6. These values must be taken as indicative since there was a large scatter in the results.

Load cells and wave probes were arranged as shown in Fig. 2 to measure, respectively, the wave height and the tension in the cables. The length of the cables with load cells was shortened to accommodate the length of the load cells and the accessories used to link them to the cables. Including the accessories, the load cells were 0.046 m long, had a mass of only 0.0141 ± 0.0001 kg and their signal cables were quite thin and flexible, so their influence on the mooring system can be neglected. Due to the S-type construction, the effects of the water pressure on the readings of the load cells was minimal.

An optical motion tracking system was used to measure and record the rigid body motion of the buoy, referenced to the centre of floatation. All three different types of records (surface elevation, tension force and motion) were synchronised and recorded with an acquisition frequency of 100 Hz.

Table 7 presents the mean values of the tension for the three configurations in rest position. The equilibrium drafts of the buoy for each test condition are listed in Table 8. The draft values include the effect of weight of the three adapters used to attach the cables, even in the free buoy condition.

The waves generated were long-crested, propagating in a direction parallel to the plane of the leeward mooring cable, Fig. 2. In this situation, the sway, roll and yaw degrees of freedom do not have significant excitation forces and the motion of the buoy is effectively reduced to surge, heave and pitch.

2.3. Test cases

Three types of tests were conducted: (i) decay tests, to determine the resonance periods of the buoy-mooring system; (ii) regular wave tests, to determine the response amplitude operators (RAO) and non-linear effects due to incident wave height; and (iii); irregular wave tests, to assess the behaviour of the mooring configurations in operational and survival conditions.

The decay tests were performed by displacing the buoy from its equilibrium position in surge, heave and pitch (one degree of freedom at a time) and then releasing the buoy. Each test was repeated at least fifteen times to reduce the uncertainty in the measurements.

In the regular wave tests, waves were generated with twenty different periods ranging from 0.8 s to 2.33 s. Around the expected resonance peaks of the system, the periods of the waves were closely spaced in order to obtain a good resolution. This was done for the target wave heights of $H = 0.04$ m and $H = 0.08$ m, to study non-linear effects due to the wave height. The tests lasted 270 s in order to record at least 100 waves for the longest period and to allow the initial transients to die out.

The irregular wave tests used the sea-states mentioned in Table 1 and each one was run for 1575 s. The duration of the irregular sea-states satisfied both the scaled down duration of a three hour sea-state as recommended in [16] (1080 s using Froude similarity with $\lambda_l = 1/100$) and the criteria of spectral analysis to obtain sufficiently resolved spectra. A JONSWAP spectrum was used for the generation of the sea-states with a shape parameter $\gamma = 3.3$. The use of this spectrum is recommend in [16], because it leads to waves with greater steepness than, for example, the Pierson–Moskowitz spectrum. Since a pseudo-random method was used to generate the irregular sea-states, the length of the sea-state cycle was set to be 1843 s, the smallest possible duration that the wave generator could create that would not be smaller than the test duration.

Table 3
Properties of the floaters. D – diameter. Indexes 1, 2 and 3 refer to the cable where the floater is installed.

	Mass (kg)	Buoyancy (N)	D (m)
F1	0.252 ± 0.001	9.97 ± 0.06	0.135 ± 0.003
F2	0.276 ± 0.001	10.05 ± 0.06	0.135 ± 0.003
F3	0.232 ± 0.001	9.96 ± 0.06	0.135 ± 0.003

Table 4
Properties of the clumpweights. Indexes 1, 2 and 3 refer to the cable where the clumpweight is installed.

	Mass (kg)	Submerged weight (N)
S1	1.0161 ± 0.0001	9.97 ± 0.06
S2	1.0246 ± 0.0001	10.05 ± 0.06
S3	1.0152 ± 0.0001	9.96 ± 0.06

Table 5
Properties of the chain. m_l – mass per unit length; γ_l – submerged weight per unit length.

Stiffness	$(1.6 \pm 0.7) \times 10^6$ N
m_l	0.1447 ± 0.0001 kg/m
γ_l	1.243 ± 0.006 N/m
Link inner length	$(2.064 \pm 0.007) \times 10^{-2}$ m
Link inner width	$(5.72 \pm 0.07) \times 10^{-3}$ m
Link thickness	$(2.99 \pm 0.05) \times 10^{-3}$ m

Table 6
Properties of the synthetic cables. m_l – mass per unit length; γ_l – submerged weight per unit length.

Stiffness (N)	m_l (kg/m)	γ_l (N/m)
$(1.6 \pm 0.3) \times 10^5$	$(3.2 \pm 0.2) \times 10^{-4}$	$(8.0 \pm 0.2) \times 10^{-3}$

Table 7
Mean tension in the cables in rest position, τ_{Stat}.

	CON1	CON2	Catenary
Cable 1	2.8 ± 0.2 N	10.6 ± 0.2 N	3.0 ± 0.2 N
Cable 2	3.1 ± 0.2 N	11.0 ± 0.2 N	3.1 ± 0.2 N

Table 8
Draft of the buoy for each configuration.

	Free	CON1	CON2	Cat.
Draft ($\pm$0.003 m)	0.174	0.175	0.186	0.178

Still in accordance with the recommendations proposed in [16], the execution of both regular and irregular sea-states was conducted in a random order to minimise bias effects. In addition, some regular sea-states were repeated to assess the repeatability of the experiments.

2.4. Data analysis

Time domain analysis of the data was performed using zero down-crossing for the surface elevation, for heave and for pitch, and mean value down-crossing for surge and for the tension, as indicated in [13]. The crossing time instant was determined by linear interpolation, while the time instants and values of the peaks were interpolated using a parabolic fit. Noise in the records was removed prior to the analysis using a zero-phase moving average filter, with seven points for the surface elevation records, five points for the position records and nine to twelve points for the tension records. These parameters were verified not to induce an unacceptable loss of amplitude of the signals. Waves or oscillations with less than 10 points (0.1 s) were not recognized as individual oscillations and were instead merged with the previous oscillation longer than 10 points (0.1 s).

The natural periods of the modes of motion were estimated from the free oscillation records obtained in the decay tests. For each test, the time elapsed between the first and the last crest and between the first and the last trough was measured, and then divided by the number of cycles encompassed by those time spans. The average of all the periods for each mode of motion was taken as the best estimate for the natural period.

The computation of the response amplitude operators was carried out using a modification of the method described in [3]. The regular wave records were filtered using a windowed-sinc filter with a Blackman window [17], to remove all

components with periods above 3.25 s, effectively removing any slowly varying oscillations and drift trends. Afterwards, an FFT of the filtered record was taken and the amplitude and frequency of the first order component extracted. These were then used as a first guess in an iterative least-squares fitting algorithm looking for the phase, frequency and amplitude that best fit the signal around that first guess. The quality of the fit was measured by the coefficient of determination.

The variance spectrum of the surface elevation was determined using Welch's method with a Hann window and 50% overlap between sub-series [18]. The initial portion of the record with the transients was removed and the data was filtered with a windowed-sinc filter to eliminate all frequency components above 10 Hz. The record was then split into 31 sub-series around 97 s long to obtain a spectral resolution of 0.01 Hz (the exact value varies from record to record depending on the length of the transient portion) and estimates with a standard deviation of 18.4% of the mean, as recommended in [16]. In the computation of the spectral parameters, the spectra were interpolated using zero-padding to a 65536 point FFT. The peak frequency was determined using the centroid method proposed in [19].

3. Results and discussion

3.1. Decay tests

Table 9 lists the resonance periods of the buoy determined experimentally for the three configurations tested and for the buoy floating freely. Even though it is not strong, there is some influence of the mooring system in the natural periods of the buoy.

The surge resonance period is smaller for CON1 than for CON2 or for the catenary. This is probably caused by the fact that the tension force at the buoy in CON1 is almost horizontal and contributes fully to the surge stiffness. Additionally, the real and added masses of CON1 are smaller than for CON2 and for the catenary, since its mooring components weigh less, are smoother and are thinner.

CON1 has the least effect on the heave motion and CON2 has the most effect. Since in CON1 the segments of the cables attached to the buoy are almost horizontal, they transmit small vertical forces to the buoy. On the other hand, in CON2 and in the catenary, the heavier and bulkier moorings increase the inertia and damping of the system, increasing the resonance period.

The pitch motion is more influenced by CON1 than by CON2 or by the catenary. This is probably due to the additional stiffness generated by the mooring system being partially compensated in CON2 and in the catenary by the increased inertia.

As suggested in [16], the peak period of the extreme sea-state SURV1 is close to the resonance periods of the buoy, leading to high loads and displacements. The operational sea-states, however are not close to the resonance periods of the buoy. This reflects the fact that, unless good control strategies are developed, a device will not always be able to operate in the most favourable sea-states for power extraction. In the particular case of the region modelled in this study, there would be at least two important operating conditions (OP1 and OP2) and the device cannot have optimal performance at both of them.

3.2. Regular waves

The results of the regular wave tests are presented in Fig. 4 in the form of RAOs for the studied modes of motion.

The surge and heave motions were non-dimensionalised by the incident wave amplitude a and the pitch motion was non-dimensionalised by the wave slope ak, where k is the wave number.

Both the type of mooring system and the wave height have an influence on the response of the buoy, but the effect of the wave height is clearly dominant. The increase in wave height causes a decrease in the response that varies between 10% and 40%, depending on the mode of motion and on the mooring configuration: the impact is greater in pitch and more moderate in heave.

Overall, the differences between the configurations are small for all modes of motion, especially outside the resonance region (as would be expected). CON1 has the highest response amplitudes in heave for all periods, and in surge and pitch for periods below the resonance. CON2 has the highest response in surge for periods longer than the heave-pitch resonance; the catenary performs slightly better than the compact configurations for some of the longer periods in pitch. The difference in the responses due to wave height and mooring configuration is always more prominent in the resonance region.

The noticeable decrease of the magnitude of the RAOs with the increase of the wave height is probably caused by the non-linear wave-body interaction, viscous damping and stiffness of the mooring systems. In the case of the viscous drag, the force increases with the square of the relative water velocity. The stiffness depends on the mean position of the buoy, which

Table 9
Natural periods of the buoy.

Degree of freedom	Free	CON1	CON2	Cat.
Surge (±0.007 s)	–	8.561	9.215	9.137
Heave (±0.007 s)	1.112	1.118	1.132	1.130
Pitch (±0.007 s)	1.170	1.145	1.168	1.163

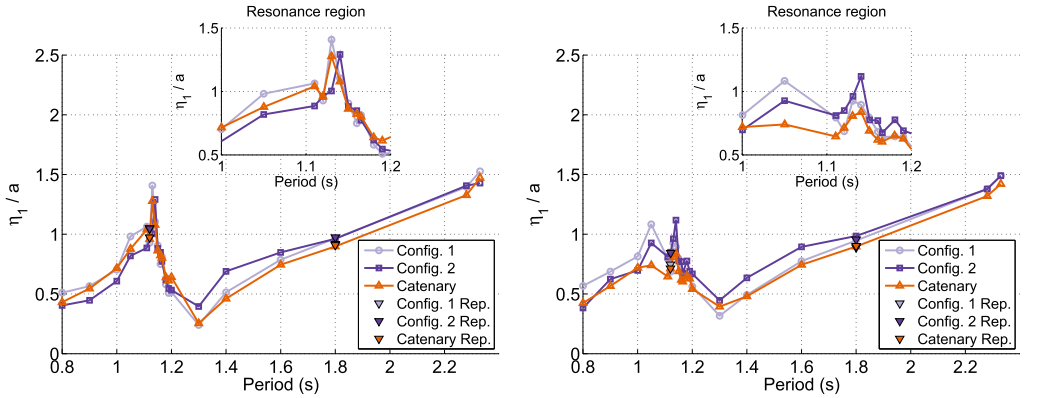

(a) Surge, $H = 0.04\,\mathrm{m}$. (b) Surge, $H = 0.08\,\mathrm{m}$.

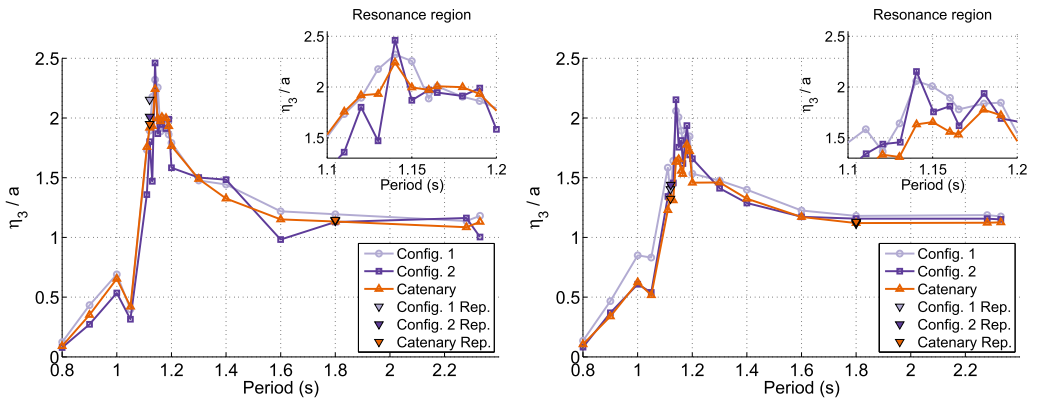

(c) Heave, $H = 0.04\,\mathrm{m}$. (d) Heave, $H = 0.08\,\mathrm{m}$.

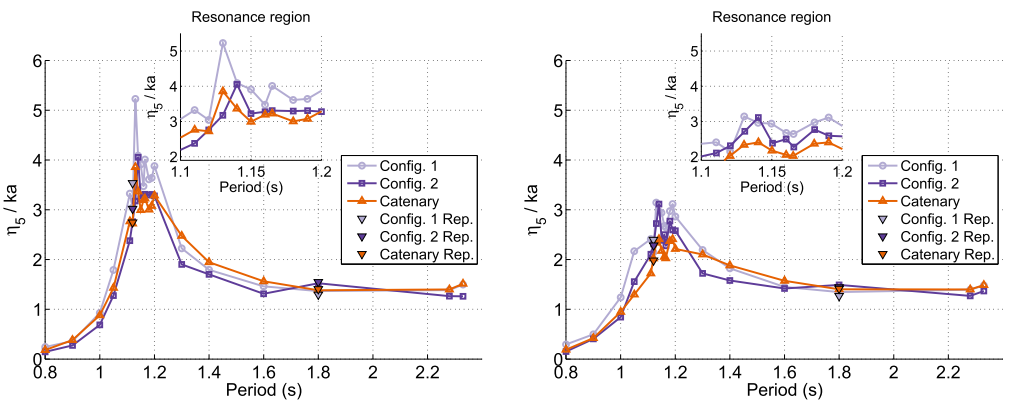

(e) Pitch, $H = 0.04\,\mathrm{m}$. (f) Pitch, $H = 0.08\,\mathrm{m}$.

Fig. 4. Response amplitude operators (RAOs) for surge, heave and pitch. Repeated test results are included as single ▽.

increases with the square of the wave height, Table 10. These effects cause relatively larger motion constraints for larger waves when compared with smaller ones.

Fig. 5 presents the relative dynamic tension (average maximum tension minus the mean tension, divided by the wave height) for the tested wave heights and mooring configurations. The plots show that, in general, the relative dynamic tension increases with the wave height, demonstrating the non-linear growth behaviour mentioned in the previous paragraph. The actual dynamic tension for 0.08 m waves is, therefore, more than the double of the dynamic tension for 0.04 m waves. The only exception occurs for CON1 at the very resonance peak.

Table 10
Mean drift of the buoy in regular waves.

T (s)	Drift (m)					
	$H = 0.04$ m			$H = 0.08$ m		
	CON1	CON2	Cat.	CON1	CON2	Cat.
0.80	0.031	0.038	0.034	0.161	0.131	0.139
0.90	0.026	0.019	0.021	0.087	0.072	0.074
1.05	0.017	0.012	0.017	0.135	0.101	0.096
1.11	0.047	0.047	0.043	0.183	0.207	0.144
1.12	0.048	0.053	0.045	0.163	0.222	0.139
1.14	0.027	0.045	0.035	0.097	0.140	0.106
1.16	0.030	0.040	0.033	0.120	0.154	0.121
1.18	0.019	0.027	0.025	0.097	0.129	0.113
1.20	0.018	0.026	0.029	0.082	0.114	0.101
1.40	-0.000	0.001	0.001	0.002	0.012	0.013
1.80	-0.002	0.004	0.000	-0.005	0.012	0.003

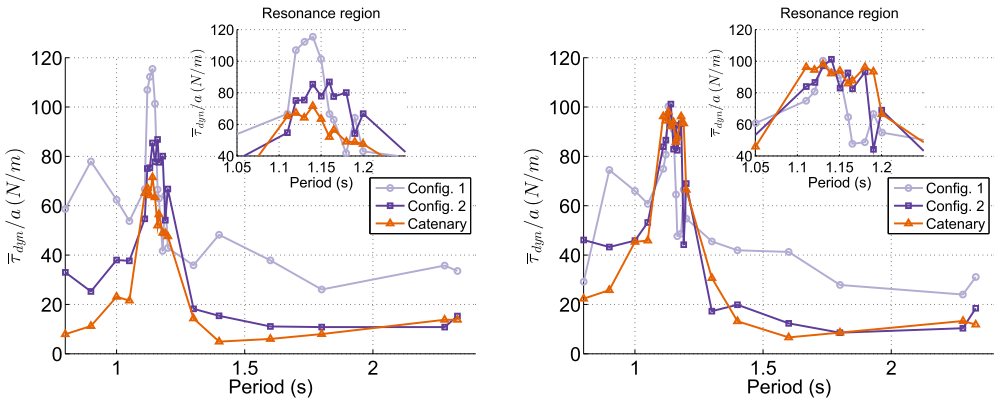

Fig. 5. Mean dynamic tension in the seaward cable in regular waves.

It can also be seen in Fig. 5 that the relative dynamic tension in CON1 has a smaller variation with the wave height than in CON2 or in the catenary. This is probably due to the segments of the mooring cables attached to the buoy in CON1 being almost horizontal and, therefore, less sensitive to the vertical movements generated in heave and pitch when in resonance. Outside of the resonance region, the motions of the buoy are slower and its amplitudes are smaller, resulting in similar relative dynamic tensions for both wave heights. The slightly higher tension values for the shorter periods in 0.08 m waves when compared to 0.04 m waves are probably due to the higher drift forces pushing the buoy to a position where the stiffness of the mooring system is higher.

Some variability in the results might be explained by the subjective criteria used to select stable intervals for analysis in tests where waves, motions or tensions forces did not get to a steady periodic state.

3.3. Irregular sea-states

Tables 11 and 12 summarise the most important results obtained in the irregular waves tests. The measured significant wave heights and peak periods are slightly different from the target values, but, since they are practically constant for all configurations, this will not have a significant impact in the results.

Using the mean squared velocity of the motions as an estimate of the average power extracted, we can see that in the operational sea-states, CON1 has always the best performance. CON2 has the second best performance, being surpassed by the catenary only in the sea-state OP1, in surge and heave. However, in these cases, the difference in performance between the CON2 and the catenary is extremely small.

To ensure the integrity of power lines or similar components, as well as to avoid possible crashes between devices, an important parameter is the maximum surge displacement in extreme seas. In this aspect, there is no configuration that is better than the others: in sea-state SURV1, the catenary has the smallest value of maximum surge displacement and CON2 has the highest; in the sea-state SURV2, CON1 has the lowest maximum surge displacement and CON2 has again the highest. It can be argued that CON2 has the worst performance. However, the maximum surge displacement of CON2

Table 11
Results from operational sea-state tests. τ – tension; η_1 – surge; η_3 – heave; η_5 – pitch; *p.p* – peak-to-peak amplitude. Overbar denotes mean value.

Parameter	OP1			OP2		
	CON1	CON2	Cat.	CON1	CON2	Cat.
H_s (m)	0.031	0.031	0.029	0.034	0.033	0.033
T_P (s)	0.90	0.90	0.90	1.28	1.28	1.30
$\overline{\eta}_1$ ($\cdot 10^{-3}$ m)	6.1	5.3	5.6	4.8	4.3	4.6
$\overline{\eta}_{1p.p}$ ($\cdot 10^{-3}$ m)	19.8	18.1	16.1	19.6	20.0	17.5
$\overline{\eta^2}_1$ (m^2/s^2)	0.064	0.059	0.060	0.088	0.085	0.073
$\max \eta_1$ ($\cdot 10^{-3}$ m)	46.2	43.8	43.3	47.4	43.6	40.0
$\overline{\eta}_{3p.p}$ ($\cdot 10^{-3}$ m)	9.1	8.5	8.5	25.3	25.1	24.5
$\overline{\eta^2}_3$ (m^2/s^2)	0.048	0.039	0.040	0.271	0.263	0.250
$\max \eta_3$ ($\cdot 10^{-3}$ m)	13.5	13.5	13.0	35.6	34.3	33.0
$\overline{\eta}_{5p.p}$ (°)	3.8	3.4	3.2	9.1	8.5	7.8
$\overline{\eta^2}_5$(rad^2/s^2)	2.3	1.8	1.6	11.0	9.5	7.8
$\max \eta_5$ (°)	5.4	4.9	4.5	10.7	10.2	9.1
$\overline{\tau}_1$ (±0.2 N)	2.9	10.8	3.1	2.9	10.7	3.1
$\max \tau_1$ (±0.2 N)	5.8	11.9	3.6	5.1	12.1	3.9
$\min \tau_1$ (±0.2 N)	0.2	9.6	2.7	0.7	9.2	2.4
τ_{Dyn1} (±0.3 N)	2.9	1.1	0.5	2.2	1.5	0.8
$\overline{\tau}_2$ (±0.2 N)	3.0	11.1	3.0	3.0	11.1	3.0
$\max \tau_2$ (±0.2 N)	6.6	12.3	3.6	5.9	12.6	3.8
$\min \tau_2$ (±0.2 N)	0.1	9.9	2.5	0.3	9.3	2.0
τ_{Dyn2} (±0.3 N)	3.6	1.2	0.6	2.9	1.6	0.8

Table 12
Results from survival sea-state tests. τ – tension; η_1 – surge; η_3 – heave; η_5 – pitch; p.p – peak-to-peak amplitude. Overbar denotes mean value.

Parameter	SURV1			SURV2		
	CON1	CON2	Cat.	CON1	CON2	Cat.
H_s (m)	0.083	0.084	0.082	0.094	0.096	0.093
T_P (s)	1.16	1.16	1.16	1.39	1.39	1.39
$\overline{\eta}_1$ ($\cdot 10^{-3}$ m)	62.5	63.2	63.6	31.9	39.0	39.6
$\overline{\eta}_{1p.p}$ ($\cdot 10^{-3}$ m)	131.2	135.2	119.5	81.7	92.8	90.0
$\max \eta_1$ ($\cdot 10^{-3}$ m)	311.6	318.6	278.7	186.8	222.7	210.8
$\max \eta_{1p.p}$ ($\cdot 10^{-3}$ m)	428.5	442.0	348.9	247.5	286.8	255.3
$\overline{\eta}_{3p.p}$ ($\cdot 10^{-3}$ m)	71.6	69.6	66.6	74.8	70.7	71.6
$\max \eta_3$ ($\cdot 10^{-3}$ m)	87.2	83.4	77.6	108.9	98.5	100.9
$\max \eta_{3p.p}$ ($\cdot 10^{-3}$ m)	171.7	164.3	154.8	198.4	183.1	183.0
$\overline{\eta}_{5p.p}$ (°)	21.8	19.1	18.0	17.6	14.8	15.5
$\max \eta_5$ (°)	25.7	22.2	20.7	21.3	17.4	18.8
$\max \eta_{5p.p}$ (°)	44.6	38.7	37.1	40.2	34.0	35.1
$\overline{\tau}_1$ (±0.2 N)	3.6	11.2	3.8	3.2	11.0	3.4
$\max \tau_1$ (±0.2 N)	11.0	17.3	17.5	9.6	14.8	11.2
$\min \tau_1$ (±0.2 N)	0.0	6.5	0.2	0.0	7.8	0.3
τ_{Dyn1} (±0.3 N)	7.4	6.2	13.7	6.4	3.9	7.8
$\overline{\tau}_2$ (±0.2 N)	2.3	10.5	2.4	2.6	10.7	2.6
$\max \tau_2$ (±0.2 N)	8.9	15.1	8.6	8.0	13.6	6.6
$\min \tau_2$ (±0.2 N)	0.0	5.7	0.5	0.0	7.1	0.7
τ_{Dyn2} (±0.3 N)	6.5	4.6	6.2	5.4	2.8	4.0

is, in both extreme sea-states, almost the same as that of the second best configuration (0.319 m vs 0.312 m in sea-state SURV1 and 0.223 m vs 0.211 m in the sea-state SURV2).

The maximum peak-to-peak amplitudes of all the motions in survival conditions provide information on possible extreme loads in the power take-off. In this aspect, the catenary is generally better than CON1 and CON2. CON1 and CON2 are better than the catenary only in the sea-state SURV2 in surge and pitch, respectively. But again, the differences between the best and the second best configuration are small.

For the purpose of safe station-keeping, the critical factor is the maximum tension in the most loaded mooring cable, which occurs, for all configurations, in sea-state SURV1 in the seaward cables (cable 1 and 3). CON1 clearly out-performs CON2 and the catenary, having a maximum tension of 11.0 N, around 57% that of CON2, 17.3 N, and of the catenary, 17.5 N.

Another important factor is the ability of the configurations to keep the cables under tension and avoid snap loads. This can be evaluated by the dynamic tension (absolute maximum tension minus the mean tension) and the minimum tension. Although it has the highest pre-tension, CON2 has the lowest dynamic tensions: 6.2 N for the sea-state SURV1 and 3.9 N for the sea-state SURV2. The highest values of dynamic tension belong to the catenary: 13.7 N for the sea-state SURV1 and 7.8 N for the sea-state SURV2. CON2, with its high pre-tension (10.6 N to 11.0 N, Table 7), is also able to keep all the cables under tension, with minimum values of 6.5 N in the seaward cables and 5.7 N in the leeward cable. On the contrary, both in CON1 and in the catenary the tension gets as low as 0.0 N (within the uncertainty of the measurements), a problem which is more severe for CON1.

According to [13], long term damage in synthetic cables (creep rupture or stress rupture) is a function of the time under elevated tension. In this aspect, CON2, with high values of mean tension (around 11 N), is in disadvantage when compared to CON1. In the catenary, a steel chain, long term damage is due to fatigue, which depends non-linearly on the number of tension cycles and on the mean tension. It cannot be compared directly with either CON1 or with CON2.

The choice of the best configuration depends on other factors, such as the variability of the weather conditions, restrictions related to the impact of certain types of anchors or mooring configurations on the seabed, etc. In sheltered regions or in regions where the difference between operational and survival conditions is not very large, CON1 might perform better than in the tests presented here, when it comes to keeping the cables under tension. The type of soil might hinder the use of drag embedment anchors or anchors resisting vertical loads, which would not allow some of the configurations to be used at all.

Overall, CON1 stands out as a good choice to maximize power production. CON2, being a hybrid between a compact configuration such as CON1 and a heavy configuration such as the catenary, combines the strong points from both of them. It seems to be a good compromise solution, reducing just a bit the possible power to be extracted when compared with CON1. The results of the catenary are close or equal to those of CON2. The power extraction is not significantly lower than in CON1, but it generates higher dynamic tensions and it takes a large amount of space, which is its main weakness.

In this study the cables were connected to the buoy around its perimeter, but the position of the attachment points is also an important variable in the dynamic behaviour of wave energy converters. Attaching all the cables to a single point on the device would decouple the pitch motion from the horizontal motions of the mooring cables, which could improve the power extraction in pitch for CON2 and for the catenary.

In [10] a single mooring configuration, similar to CON1, was tested in an array of devices with power take-off using short-crested waves. The results showed that short-crested waves and array configurations will lead to higher peak loads in the mooring cables. So, although the results presented here are relevant to compare different configurations, it is also important to assess the dynamics of the mooring system in more complex set-ups.

4. Conclusion

Different mooring configurations for wave energy converters were tested in physical models and the results presented. The configurations were (i) a compact mooring arrangement composed of a synthetic cable with an intermediate floater; (ii) a compact mooring configuration composed of a synthetic cable with a floater and a clumpweight, creating a zig–zag pattern; and (iii) a catenary.

The parameters analysed included those common in the design of typical mooring systems, but also parameters more relevant to wave energy converters, such as the mean square value of the velocities (to estimate power extraction) or the peak-to-peak amplitudes (to estimate extreme loads in the power take-off).

The configuration using synthetic cables with an intermediate floater (CON1) provided the best results for power extraction and had the least interference in the heave mode of motion (where its natural period was almost the same as for the buoy floating freely). This happened because the vertical motion of the wave energy converter was decoupled from the motions of the mooring cables. However, this configuration was not so good at maintaining tension in the cables under extreme conditions.

The configuration with a floater and a clumpweight (CON2) had a slightly worse performance than the one with only the floater when it came to power extraction. It was the best configuration at keeping the cables under tension while at the same time minimizing the dynamic tension. It had also the smallest impact in the natural period of the pitch mode of motion.

The catenary had a good performance in extreme sea-states, where it limited the maximum surge displacement and the peak-to-peak amplitudes of surge, heave and pitch. In the operational sea-states, it had the lowest performance in power extraction. It had also, by far, the largest footprint of the three configurations, which leads to increased costs and environmental impact. Still, even though it has not been specially designed for wave energy converters, it might have an acceptable performance, depending on the working principle and on how it is attached to the device.

In spite of the ranking of each configuration for each parameter, the differences between the configurations were not large in any situation.

The presented results did not contain any sensitivity analysis of the parameters of the compact configurations, but this data will be the subject of future publications.

On a final note, seemingly contradictory results and conclusions regarding the quality of different mooring systems may be perfectly compatible, since they depend on the studied situation, on how the problem is analysed and on the parameters deemed to be relevant.

Acknowledgments

This work was funded by the Portuguese Foundation for Science and Technology (FCT – Fundação para a Ciência e Tecnologia) through the research Grant SFRH/BD/62040/2009 and the POPH/FSE program and by Adlerbertska research fund in Gothenburg, Sweden.

References

[1] N. Fonseca, R. Pascoal, T. Morais, R. Dias, Design of a mooring system with synthetic ropes for the FLOW wave energy converter, in: Proceedings of the ASME 2009 28th International Conference on Ocean, Offshore and Arctic Engineering, part b edition, vol. 4, American Society of Mechanical Engineers, Honolulu, HI, United states, 2009, pp. 1189–1198.
[2] E. Angelelli, B. Zanuttigh, F. Ferri, J. Kofoed, Experimental assessment of the mooring influence on the power output of floating wave activated body WECs, in: P. Frigaard, J.P. Kofoed, A.S. Bahaj, L. Bergdahl, A. Clément, D. Conley, A.F.O. Falcão, C.M. Johnstone, L. Margheritini, I. Masters, A.J. Sarmento, D. Vicinanza (Eds.), Proceedings of the 10th European Wave and Tidal Energy Conference, European Wave and Tidal Energy Conference, Aalborg, Denmark, 2013.
[3] V. Harnois, S. Weller, L. Johanning, P. Thies, M. Le Boulluec, D. Le Roux, V. Soulé, J. Ohana, Numerical model validation for mooring systems: method and application for wave energy converters, Renew. Energy 75 (2015) 869–887, http://dx.doi.org/10.1016/j.renene.2014.10.063.
[4] P. Vicente, A.D.O. Falcão, P. Justino, Non-linear slack-mooring modelling of a floating two-body wave energy converter, in: Proceedings of the 9th European Wave and Tidal Energy Conference, European Wave and Tidal Energy Conference, Southampton, 2011.
[5] J. Fitzgerald, L. Bergdahl, Considering mooring cables for offshore wave energy converters, in: Proceedings of the 7th European Wave and Tidal Energy Conference, IST/IDMEC, Porto, 2007.
[6] F. Cerveira, N. Fonseca, R. Pascoal, Mooring system influence on the efficiency of wave energy converters, Int. J. Mar. Energy 3–4 (2013) 65–81, http://dx.doi.org/10.1016/j.ijome.2013.11.006.
[7] J. Tedd, E. Friis-Madsen, J.P. Kofoed, W. Knapp, Wave dragon, in: J. Cruz (Ed.), Ocean Wave Energy – Current Status and Future Perspectives, first ed., Springer-Verlag, Berlin, Heidelberg, 2008, pp. 321–336, http://dx.doi.org/10.1007/978-3-540-74895-3 (Chapter 7.4).
[8] J. Fitzgerald, L. Bergdahl, Including moorings in the assessment of a generic offshore wave energy converter: a frequency domain approach, Mar. Struct. 21 (1) (2008) 23–46, http://dx.doi.org/10.1016/j.marstruc.2007.09.004.
[9] J. Falnes, Ocean Waves and Oscillating Systems, Cambridge University Press, Cambridge, 2002.
[10] V. Krivtsov, B. Linfoot, Basin testing of wave energy converters in Trondheim: investigation of mooring loads and implications for wider research, J. Mar. Sci. Eng. 2 (2014) 326–335, http://dx.doi.org/10.3390/jmse2020326.
[11] L. Bergdahl, Wave-Induced Loads and Ship Motions, Chalmers University of Technology, Göteborg, 2010.
[12] M. Costa, R. Silva, J.A. Vitorino, Contribuição para o estudo do clima de agitação maŕtima na costa portuguesa, in: 2as Jornadas Portuguesas de Engenharia Costeira e Portuária, AIPCN/PIANC Secção Portugal, Sines, 2001.
[13] Det Norske Veritas, Offshore Standard DNV-OS-E301 – position mooring, 2004.
[14] N. Barltrop, Floating Structures – A Guide for Design and Analysis, vol. 2, Energy Institute, 1998.
[15] S.K. Chakrabarti, Offshore Structure Modeling, World Scientific Publishing Co., Singapore, 1994.
[16] Equimar, Protocols for the Equitable Assessment of Marine Energy Converters, first ed., The Institute for Energy Systems, School of Engineering, The University of Edinburgh, Edinburgh, 2011.
[17] S.W. Smith, The Scientist and Engineer's Guide to Digital Signal Processing, California Technical Publishing, San Diego, 1997.
[18] P. Welch, The use of fast Fourier transform for the estimation of power spectra: a method based on time averaging over short, modified periodograms, 1967. doi: http://dx.doi.org/10.1109/TAU.1967.1161901.
[19] IAHR Working Group on Wave Generation and Analysis, List of sea-state parameters, J. Waterway Port Coastal Ocean Eng. 115 (6) (1989) 793–808.